Sawamura D, Abe R, Goto M, Akiyama M, Hemmi H, Akira S, Shimizu H	Direct injection of plasmid DNA into the skin induces dermatitis by activation of monocytes through toll-like receptor 9.	**J Gene Med**	17	17	2005
Yasukawa K, Sawamura D, Akiyama M, Motoda N, Shimizu H	Keratotic lesions in *epidermolysis bullosa simplex* with mottled pigmentation.	**J Am Acad Dermatol**	52	172-173	2005

Regulation of Human Melanoma Growth and Metastasis by AGE–AGE Receptor Interactions

Riichiro Abe,* Tadamichi Shimizu,* Hiroshi Sugawara,* Hirokazu Watanabe,* Hideki Nakamura,* Hiroshi Choei,† Nobuyuki Sasaki,† Sho-ichi Yamagishi,‡ Masayoshi Takeuchi, and Hiroshi Shimizu*

*Department of Dermatology, Hokkaido University Graduate School of Medicine, Sapporo, Japan; †Department of Neuropsychiatry, Sapporo Medical University, Sapporo, Japan; ‡Department of Medicine, Kurume University School of Medicine, Kurume, Japan; Department of Biochemistry, Faculty of Pharmaceutical Science, Hokuriku University, Kanazawa, Japan.

Advanced glycation end products (AGE), nonenzymatically glycated protein derivatives, have been implicated in the development and progression of diabetic angiopathies, including skin dermopathy. Nevertheless, the involvement of AGE in the development and progression of melanoma has not been fully elucidated. In this study we investigated the expression levels of their receptor for AGE (RAGE) in human melanoma and subsequently studied the effects of AGE on melanoma growth and migration. First, RAGE was detected in the cytoplasm of human melanoma cells (G361 and A375). Among the different types of AGE, glyceraldehyde- and glycolaldehyde-derived AGE significantly stimulated the growth and migration of human melanoma cells. Furthermore, tumor formation of melanoma cell xenografts in athymic mice was prevented by treatment with anti-RAGE neutralizing antibodies. In tumor-bearing mice, survival rates were prolonged, and spontaneous pulmonary metastases were inhibited by treatment using anti-RAGE neutralizing antibodies. In addition, all AGE were present in beds of human melanoma tumor, whereas they were barely detected in normal skin. These results suggest that AGE might be involved in the growth and invasion of melanoma through interactions with RAGE and represent promising candidates for assessing the future therapeutic potential of this therapy in treating patients with melanoma.

Key words: migration/invasion.
J Invest Dermatol 122:461–467, 2004

The main cause of treatment failure and death for cancer patients is metastasis—the formation of secondary tumors in organs a long way from the original cancer. Among cancers, melanoma is the most highly invasive and metastatic tumor with an incidence and mortality that have been rapidly increasing above those of any other cancers in recent year (Morton *et al*, 1993). Adjuvant therapy of proven efficacy is not currently available for these patients; therefore, the search for new targets for therapeutic reagents is required to prevent both proliferation and metastasis. Nevertheless, the molecular and genetic events that contribute to the formation and progression of cutaneous melanoma are poorly understood. It has been reported that oxidative stress contributes to the pathogenesis of melanoma. Indeed, ultraviolet irradiation, one of the highest risk factors for melanoma (McKie, 1998; Noonan, 2001), causes oxidative DNA damage that is additionally potentially mutagenic (Setlow *et al*, 1993).

Advanced glycation end products (AGE), nonenzymatically glycated protein derivatives, were originally known to accumulate in various tissues and have been implicated in the development of diabetic vascular complications, for example, retinopathy and nephropathy (Yang *et al*, 1994; Stitt *et al*, 1997). Recent studies demonstrated that AGE synthesis is accelerated by intra- and extracellular oxide stress (Mullarkey *et al*, 1990). The receptor for advanced glycation end products (RAGE), a multiligand member of the immunoglobulin superfamily of cell surface molecules, interacts with distinct molecules implicated in homeostasis, development, and inflammation (Schmidt *et al*, 2001). Binding RAGE by a ligand triggers activation of key cell-signaling pathways, thereby reprogramming cellular properties. Recently Taguchi and colleagues (2000) have identified RAGE in a molecular checkpoint that regulates not only the invasiveness but also the growth and movement of glioma cells. Nevertheless, the role of RAGE is still unclear in melanoma proliferation and metastasis. One of the hypotheses for the pathogenesis of melanoma growth and migration suggests that AGE formed at an accelerated rate under oxidative stress conditions might be involved in the growth and invasion of melanoma through the interactions with RAGE. In addition, we have previously elucidated the pathways of AGE formation and characterized distinct AGE classes (AGE1–5) and their different cell-mediated responses (Takeuchi *et al*, 1999, 2000a, b).

The aim of this study was to investigate whether distinct AGE–RAGE interactions are a potential enhancer for growth and/or cell migration in human melanoma cell.

Abbreviations: AGE, advanced glycation end product; CML, *N*-(carboxymethyl)lysine; PBS, phosphate-buffered saline; PBS-T, PBS-Tween; RAGE, receptor for advanced glycation end product.

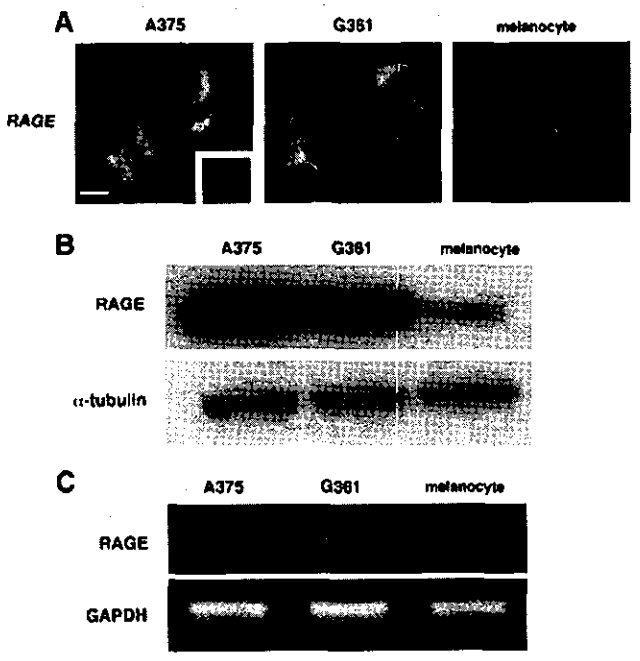

Figure 1
RAGE is expressed in human melanoma cell. (*A*) A375 and G361 melanoma cells cultured on slides were analyzed for RAGE using confocal fluorescence microscopy. Control panels indicate the staining with control IgG. *Bars*, 10 μm. (*B*) RAGE (35 kDa) and α-tubulin (50 kDa) were analyzed by western blot of melanoma cells (A375, G361) and melanocyte lysates. (*C*) RT-PCR was performed with RNA isolated from melanoma cells (A375, G361) and melanocytes and degenerate primers based on the RAGE and glyceraldehyde-3-phosphate dehydrogenase amino acid sequences.

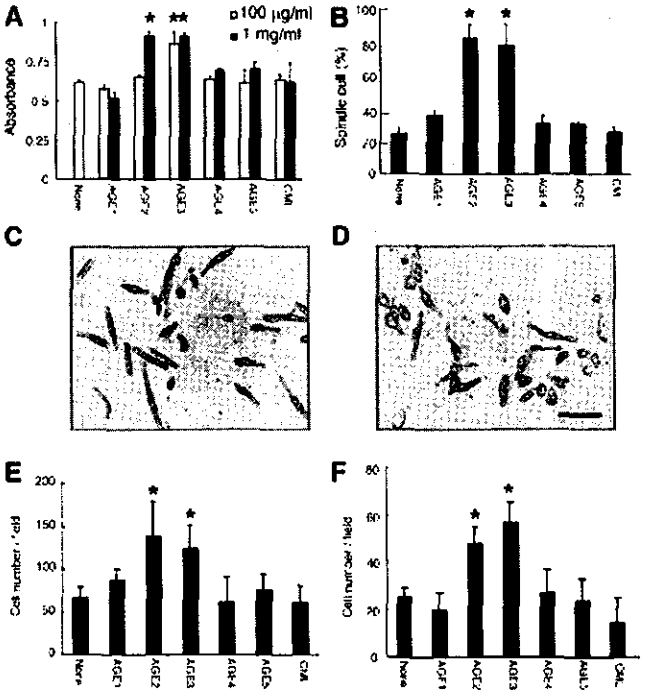

Figure 2
AGE2- and AGE3-induced melanoma cell proliferation, migration, and invasion *in vitro*. The medium of G361 melanoma cells was added each AGE or CML (100 μg/mL or 1 mg/mL) for 48 h. (*A*) Proliferation was assessed by WST-1 assay. *$p<0.01$ compared with medium alone. (*B*) G361 cells were treated with AGE (1 mg/mL) and cultured on plastic dishes coated with purified collagen I. After 18 h of incubation, cells were photographed under phase contrast microscopy. (*C*) AGE2; (*D*) no addition. *Bars*, 50 μm. *The spreading cells are counted as* spindle cells if they had a length/width ratio greater than three. *$p<0.005$ compared with medium alone. In migration and invasion assay, G361 cells were layered on top of the membrane of Transwell devices (*E*) or Matrigel-coated membrane (*F*). Cells were allowed to migrate through the membrane for 16 h (migration assay) or 48 h (invasion assay). Transmigrated cells were counted by crystal violet staining. *$p<0.005$ compared with medium alone.

Results

RAGE expressed in human melanoma cells To investigate whether RAGE *proteins are* detected in human melanoma, melanoma cell lines (G361 and A375) and normal melanocyte were immunohistochemically examined using antibodies against RAGE. The results showed the presence of RAGE protein in the membrane and cytoplasm of these melanoma cells (Fig 1*A*), which is similarly staining pattern with astrocytes (Sasaki *et al*, 2001). Melanocyte expressed RAGE weakly compared melanoma cell. This was confirmed by western blotting experiments in which RAGE (35 kDa) was detected in melanoma cell extractions, whereas normal melanocyte extraction contained lower level of RAGE (Fig 1*B*). To further confirm these RAGE expression results, quantitative analyses of RAGE mRNA expression were undertaken using RT-PCR. The results showed that RAGE mRNA (262 bp) was detected in two melanoma cell lines (Fig 1C). Nevertheless, it was barely detected in normal melanocytes. These data give a consistent representation of RAGE expression observed in the melanoma cell lines.

AGE2- and AGE3-induced cell proliferation of melanoma cells *in vitro* The next experiment determined which AGE induce melanoma cell growth *in vitro*. The immunochemically distinct AGE (AGE1, glucose-derived AGE; AGE2, glyceraldehyde-derived AGE; AGE3, glycolaldehyde-derived AGE; AGE4, methylglyoxal-derived AGE; AGE5, glyoxal-derived AGE) (Takeuchi *et al*, 1999, 2000a, b) were used. *Various concentrations* (0–1 mg/mL) of AGE were added to the culture medium of G361 cells. Cell growth was assessed using a modified MTS assay after a 48-h incubation with the added compounds. Significant growth stimulation with the addition of AGE2 and AGE3 was observed ($p<0.01$), whereas other AGE failed to enhance cell proliferation (Fig 2*A*).

AGE2- and AGE3-induced migration and invasion in melanoma cells *in vitro* Previous report indicated that RAGE mediates migration of glioma cells (Taguchi *et al*, 2000); therefore, we then *assessed these properties in* melanoma cells *in vitro*. First, we observed the morphologic changes by caused the addition of AGE, involved in their ability to extend processes necessary to migrate into the surrounding matrix. The spreading cells were counted as spindle cells if they showed a length-to-width ratio of more than 3 (Fig 2*B–D*). The population of spindle cells was 24% when G361 cells were cultured with no addition on collagen-I-coated matrix. Only AGE2 and AGE3 increased spindle cells population to 81% and 77, respectively

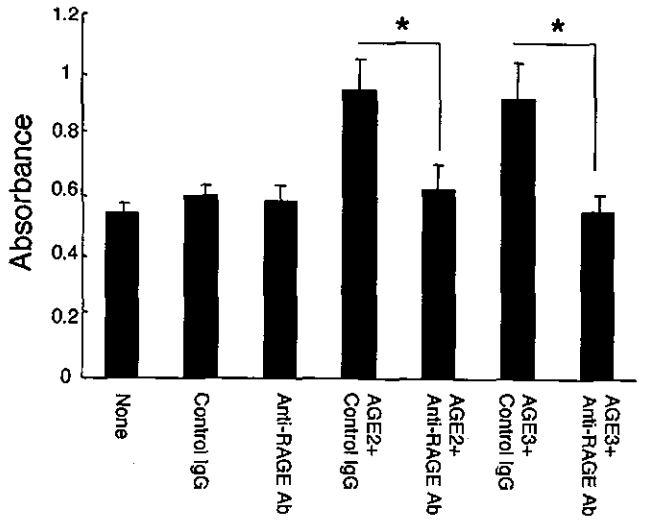

Figure 3
Anti-RAGE antibody inhibited the melanoma cell proliferation induced by AGE2 and AGE3. The medium of G361 was added with each AGE2 and AGE3 (1 mg/mL), anti-RAGE antibody (10 μg/mL), of control IgG (10 μg/mL) as indicated for 48 h at 37°C. The proliferations were assessed by WST-1 assay. *$p < 0.005$.

($p < 0.005$). To explore whether AGE enhance melanoma cell migration and invasion, G361 cells were examined in migration and invasion assays. The migration of G361 cells was significantly enhanced by 138 and 108% by AGE2 and AGE3, respectively ($p < 0.005$) (Fig 2*E*). Similarly, during invasion assays, numbers of invading cells, which were able to degradate Matrigel, also increased with the addition of AGE2 and AGE3 ($p < 0.005$) (Fig 2*F*).

Anti-RAGE antibody inhibited melanoma cell proliferation induced by AGE2 and AGE3 It was investigated whether anti-RAGE antibodies could inhibit AGE-induced melanoma cell proliferation. This antibody was shown to neutralize RAGE engagement; namely, it completely inhibited G361 cell proliferation stimulated by either AGE2 or AGE3 (Fig 3).

RAGE blockade suppressed growth of implanted melanoma in immunocompetent mouse Next we analyzed the effects of anti-RAGE antibodies on the growth of melanoma tumors using G361 melanoma xenografts *in vivo*. Initially, mice were subcutaneously injected with G361 cells into their upper flanks. After 10 d mice were treated intraperitoneally with 0.5 mg of either anti-RAGE antibody or control IgG, once every 5 d. The mouse tumors treated with the control antibody continued their aggressive growth to reach the size of 400 mm^3 by day 30 (Fig 4*A*). In contrast, treatment with anti-RAGE antibody resulted in a significant twofold reduction in tumor size compared with control IgG-treated mice ($n = 5$/group, $p < 0.01$). To determine whether RAGE tumor growth inhibition was associated with inhibition of tumor blood vessel formation, tumor fragments were processed for histologic examination. Because the number of capillaries was not different between tumor-treated anti-RAGE antibodies and control IgG (Fig 4*B,C*), this tumor

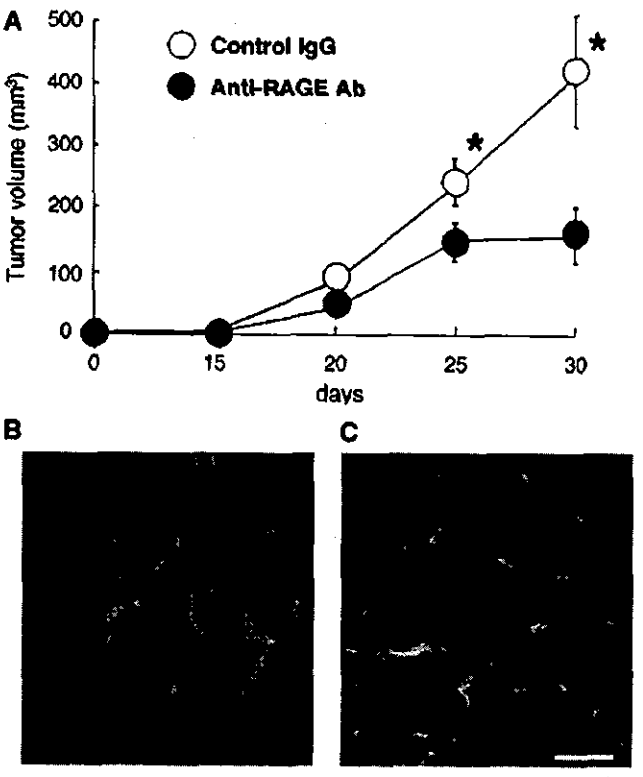

Figure 4
RAGE blockade suppressed growth of implanted G361 melanoma, not by inhibition of angiogenesis. (*A*) G361 melanoma cells (5×10^6) were injected subcutaneously into the upper flank of Balb/c-nu/nu mice ($n = 5$/group). Mice received intraperitoneal injections of PBS, control IgG (0.5 mg), or anti-RAGE antibodies (0.5 mg) after 10 d; they were injected every 5 days. Tumor weights (average ± SD) were measured. *$p < 0.01$. For immunohistochemical analysis of microvessels in the tumor tissues, sections were stained with anti-CD34 (*FITC, green*) antibody. Nuclei were stained with propidium iodide (*red*). Microvessels in the anti-RAGE antibody-treated melanoma tissues (*B*) and control IgG-treated melanoma tissue (*C*). *Bars*, 50 μm.

growth suppression was not induced by inhibition of angiogenesis.

RAGE blockade prolonged survival of tumor-bearing mice and inhibited spontaneous lung metastasis G361 cells (1×10^6) were injected intraperitoneally into nude mice to evaluate the effect of anti-RAGE antibody on the mortality rate. Mice received intraperitoneal injections of 0.3 mL of either control IgG (0.5 mg) or anti-RAGE antibody (0.5 mg) 10 d later and once every 5 d. The survival time of tumor-bearing mice injected with anti-RAGE antibody was significantly longer than tumor-bearing mice injected with control IgG ($n = 5$/group, $p < 0.05$) (Fig 5*A*).

Next, we examined whether anti-RAGE antibodies influenced metastasis *in vivo*. When the tumor volume size established by the initial G361 injection into the upper flank of nude mice reached 500 mm^3, primary tumors were excised. Mice were then maintained for an additional 3 wk to allow further growth of lung metastases. Mice received intraperitoneal injections of 0.3 mL of control IgG (0.5 mg) or anti-RAGE antibody (0.5 mg) once every 3 d after tumors were removed. The number of macroscopic surface lung colonies per mouse was used as a parameter for judging

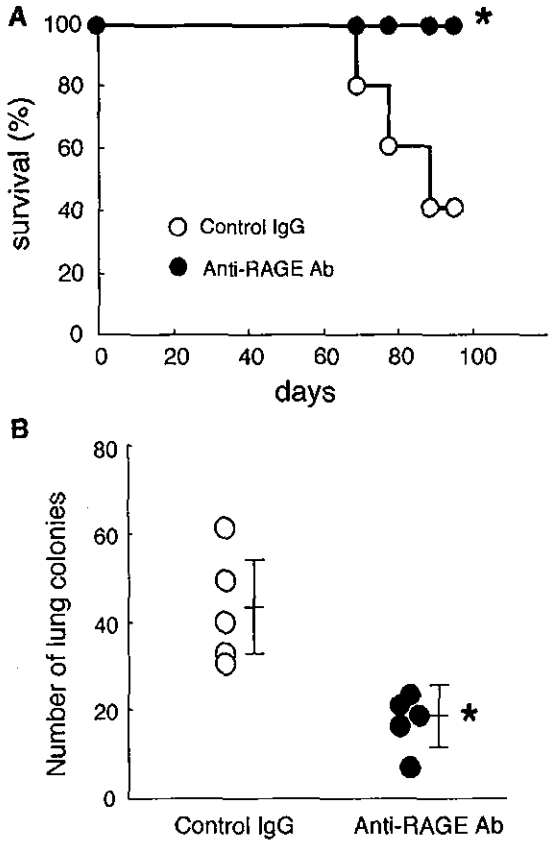

Figure 5
RAGE blockade prolonged survival of tumor-bearing mouse and inhibited spontaneous lung metastasis. (*A*) A single-cell suspension of 1×10^6 G361 melanoma cells was injected into the peritoneal cavity of 6-wk-old female athymic nude mice (n = 5/group). Mice received intraperitoneal injections of 0.3 mL of control IgG (0.5 mg) or anti-RAGE antibodies (0.5 mg) after 10 d and once per 5 days. Mice were then observed for survival, which was recorded as the percentage of surviving animals over time (in days) after tumor injection. *$p < 0.01$. (*B*) 1×10^6 G361 cells were injected into the upper flank of nude mice (n = 5/group). When the mean tumor volume reached 500 mm^3, primary tumors were removed. Mice were then maintained for an additional 3 wk to allow further growth of lung metastases. Mice received intraperitoneal injections of control IgG (0.5 mg) or anti-RAGE antibodies (0.5 mg) once every 3 d after tumors were removed. The mice were necropsied, and the lungs were removed. Visible lung metastases were counted with the aid of a dissecting microscope. *$p < 0.01$.

the lung colonization efficiency. The metastatic efficiency was markedly reduced in mice treated with anti-RAGE antibody (n = 5/group, $p < 0.05$) (Fig 5*B*).

AGE and RAGE expressed in human melanoma tissue To investigate whether AGE and RAGE proteins are detected in human melanoma *in vivo*, human melanoma specimens were immunohistochemically examined for antibodies against various types of immunochemically distinct AGE (AGE1-5), CML, and RAGE. The results showed that AGE2 was strongly present within cytoplasm of melanoma cells and in the extracellular matrix (Fig 6*A*). All of other AGE and CML were similarly stained (data not shown). In contrast, RAGE was detected only in cytoplasm of melanoma cells. In normal skin, AGE and CML were hardly detected, and also RAGE was hardly stained in melanocytes (data not shown).

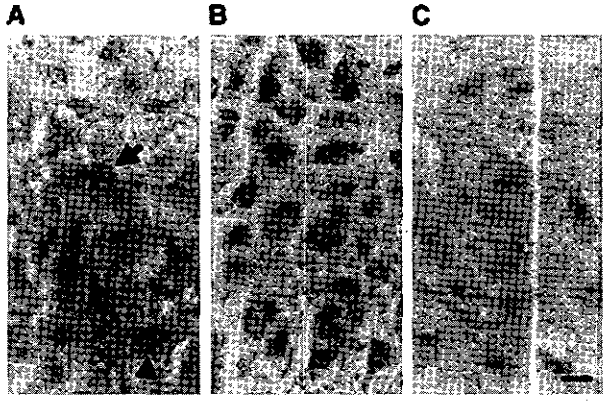

Figure 6
AGE and RAGE are expressed in human melanoma. Immunohistochemical preparations stained with anti-AGE2 (*A*), anti-RAGE (*B*), and control IgG (*C*) using the avidin-biotin immunoperoxidase method. The data of other AGE and CML were not shown. (*A, arrow*) Intracellular and (*arrowhead*) extracellular AGE2 localization. *Bars*, 10 μm.

Discussion

Here we demonstrate that RAGE was expressed in human melanoma cells. Furthermore, glyceraldehyde-derived AGE (AGE2) and glycolaldehyde-derived AGE (AGE3) enhanced proliferation, migration, and invasion of this melanoma cell line *in vitro*. Finally, the treatment by intraperitoneal injection of the neutralizing anti-RAGE antibody reduced local tumor formation, prolonged survival rate, and inhibited lung metastases in nude mice.

It has been reported that RAGE is expressed by a range of cell types, including endothelial cell, astrocytes, and some malignant cells such as malignant glioma and squamous cell carcinoma, contributing to homeostasis, development, inflammation, and carcinogenesis (Mullarkey *et al*, 1990; Yamagishi *et al*, 1997; Yamamoto *et al*, 1995; Sasaki *et al*, 1998). We and other groups have reported that AGE were present in various tissues including endothelial cells of blood vessel, mesenchymal cells, and extracellular matrix (Ling *et al*, 1998; Mizutari *et al*, 1997). Accumulation of AGE initiated various important processes including angiogenesis in diabetic microangiopathies (Yamagishi *et al*, 1997). AGE formation in the extracellular matrix of skin is accelerated by ultraviolet-induced oxidation (Mizutari *et al*, 1997), and AGE generate active oxygen species in the skin during ultraviolet irradiation (Masaki *et al*, 1997), suggesting the presence of vicious cycle of AGE formation. Furthermore, AGE can activate RAGE expression causing enhanced AGE–RAGE interaction (Tanaka *et al*, 2000). It is thus hypothesized that activated cells that include not only tumor cells but also stromal cells located in peritumor site synthesize AGE. Taken together, we hypothesize that convenient for melanoma cells proliferate and invade with abundant accumulation of extracellular AGE in skin.

We have highlighted the pathways of AGE formation and characterized distinct AGE classes (AGE1–5) with different cell-mediated responses (Takeuchi *et al*, 1999, 2000a, b). In this study, AGE2 and AGE3 but not other AGE, can upregulate melanoma cell growth, migration, and invasion *in vitro*. Recently, we also reported strong RAGE binding by

AGE2 and AGE3, but not other AGE (Yonekura *et al*, 2003). Taken together, AGE2– and AGE3–RAGE interactions have an important role in the progression of melanoma. Although previous papers reported that CML–RAGE interaction mediates cell signaling (Kislinger *et al*, 1999), our data showed CML influence little effects on melanoma proliferation, migration, and invasion. We speculate that this disparity is dependent on cell types or transformation (malignant or normal).

We also assessed the therapeutic efficacy of AGE–RAGE interactions in a xenograft model. In our experiments, blocking RAGE by the systemic administration of neutralizing RAGE antibody significantly inhibited the growth of G361 xenograft tumors and spontaneous lung metastasis. Furthermore, the blockade of RAGE prolonged the survival of G361 tumor-bearing mice. Previously we reported that this interaction could play a significant role in the progression of pancreatic cancer through the induction of autocrine platelet-derived growth factor-B (Yamamoto *et al*, 1995). Furthermore, Taguchi and associates (2000) showed that this interaction regulates not only the growth but also the movement and invasiveness of glioma tumor cells (Mullarkey *et al*, 1990). In addition, the presence of AGE was confirmed in human melanoma beds, whereas those were barely detected in normal skin, indicating that the interaction of upregulated RAGE in melanoma cells and AGE that are present in tumor beds promotes melanoma progression. We concluded that these interactions regulate various malignant tumors, which have a particularly high invasive and metastatic potential.

In conclusion, our findings have identified a pivotal role for AGE–RAGE interactions in human melanoma growth and metastasis. We suggested that blockage of these interactions, including using the anti-RAGE antibody are represent a good candidates for treatment of patients with melanoma.

Materials and Methods

Human melanoma specimens Two consecutive cases of melanoma tissue biopsies taken for routine diagnosis with patient consent and ethical permission were retrieved from the Department of Dermatology, Hokkaido University Graduate School of Medicine.

Mice and cell lines Balb/c-nu/nu mice were purchased from Japan Clea (Tokyo, Japan) and maintained under specific pathogen-free conditions. All animal procedures were conducted according to guidelines from the Hokkaido University Institutional Animal Care and Use Committee under an approved protocol. The two human melanoma cell lines, G361 and A375 (American Type Culture Collection, Manassas, VA) were maintained in RPMI 1640 supplemented with 10% fetal calf serum, 100 units per mL penicillin/streptomycin. Normal human neonatal melanocytes were purchased from Kurabo (Osaka, Japan) and were cultured according to the manufacturer's instructions.

Preparation of AGE proteins and *N*-(carboxymethyl)lysine–bovine serum albumin AGE–bovine serum albumin and AGE–rabbit serum albumin were prepared as described previously (AGE1, glucose-derived AGE; AGE2, glyceraldehyde-derived AGE; AGE3, glycolaldehyde-derived AGE; AGE4, methylglyoxal-derived AGE; AGE5, glyoxal-derived AGE) (Takeuchi *et al*, 1999, 2000a, b). Carboxymethyllysine (CML)–bovine serum albumin was prepared as described elsewhere (Ikeda *et al*, 1996). Protein concentrations were determined with the DC protein assay reagent (Bio-Rad Laboratories, Richmond, CA) using bovine serum albumin as a standard.

Preparation of antibodies A polyclonal antibody against RAGE was raised in rabbits (Sasaki *et al*, 2001). The peptides were synthesized according to the amino acid sequences of RAGE, residues 167 to 180 in extracellular domain. Synthesized peptide was coupled to keyhole limpet hemocyanin and mixed with an equal volume of Freund's complete adjuvant. The conjugated peptide were injected into rabbits three times at 2-wk intervals. Serum was obtained 2 wk after last injection, and antibody titer was assessed by ELISA. This anti-RAGE antibody certainly recognizes full-length RAGE (Sasaki *et al*, 2001). For *in vivo* experiments, the IgG fraction of antiserum was purified by Sepharose A. Antibodies specific for all AGE (AGE1–5 and CML) were prepared as previously described (Takeuchi *et al*, 1999, 2000a, b).

Immunofluorescence microscopy Immunofluorescence staining was performed on melanoma cells grown on glass coverslips. The glass coverslips were incubated with anti-RAGE antibody (1:100 dilution) overnight at 4°C in Tris-buffered saline containing 1% bovine serum albumin. The primary antibodies were detected using fluorescein isothiocyanate-labeled goat anti-rabbit IgG (Vector Laboratories, Burlingame, CA). The glass coverslips were examined using a confocal laser microscope (laser scanning confocal imaging system Model MRC 1024, Bio-Rad) equipped with an inverted fluorescence microscope (Zeiss, Germany).

Western blot G361, A375, and normal melanocytes were grown to confluence in 100-mm dishes, washed with phosphate-buffered saline (PBS), and lyzed as previously described (Shimizu *et al*, 1999). Samples containing 50 μg of protein were loaded onto 10% acrylamide gels. Proteins were separated by sodium dodecyl sulfate-polyacrylamide gel electrophoresis and electrophoretically transferred to nitrocellulose filters. After transfer, the filters were blocked by incubation with 5% nonfat dry milk in PBS-Tween (PBS-T) buffer overnight at room temperature. The filters were then incubated for 1 h with PBS-T containing 0.1% nonfat dry milk and the anti-RAGE antibody at 1:2500 dilution or α-tubulin antibody (Santa Cruz Biotechnology, Santa Cruz, CA) at 1:1000. Next, the filters were washed three times in PBS-T and incubated with PBS-T containing 0.1% nonfat dry milk and horseradish peroxidase-linked anti-rabbit Ig [$F(ab')_2$] (Amersham-Life Science, Buckinghamshire, UK) diluted 1:5000 for 1 h at room temperature. Filters were washed three more times in PBS-T, and immunoreactivity was detected using an enhanced chemiluminescence western blot detection system (Amersham), followed by exposure to ECL HYPER film (Amersham).

Reverse transcription-polymerase chain reaction In brief, PCR was carried out as previously described (Tanji *et al*, 2000). The sense primer for RAGE was from bp 1801 to bp 1820 (5′-GCCCTCCAGTACTACTCTCG-3′), and the antisense primer was from bp 2043 to bp 2062 (5′-TGTGTGGCCACCCATTCCAG-3′). The sense and antisense primers for glyceraldehyde-3-phosphate dehydrogenase (GAPDH) were from bp 204 to bp 226 (5′-CAATGGAAATCCCATCACCATCT-3′) and from bp 908 to bp 930 (5′-AATGAGCTTGACAAAGTGGTCGT-3′), respectively. The entire RT reaction product was used for PCR amplification. Forty cycles of amplification were performed using a thermal programmer (Perkin Elmer, Wellesley, MA), as follows: denaturation at 94°C for 15 s and annealing and extension at 60°C for 30 s. The PCR products were then electrophoresed on a 1.5% agarose gel stained with ethidium bromide.

Proliferation assay The cell proliferations were assessed by using a modified MTT assay, the WST-1 assay, which is a colorimetric assay based on the cleavage of the tetrazolium salt

WST-1 to a formazan dye by the mitochondrial dehydrogenase of viable cells. G361cells (5×10^3 cells per well) were preincubated for 24 h with serum-free medium at 37°C. The medium was replaced with medium containing each AGE, CML (0–1 mg/mL) or anti-RAGE antibody (10 μg/mL) and control IgG (10 μg/mL) for 48 h at 37°C. The ready-to-use WST-1 reagent (Dojin, Kumamoto, Japan) was added to the cells during the last 4 h and incubated at 37°C. Viable cells were then determined using a microplate reader at 450 nm with a 630-nm reference wavelength.

Transmigration and invasion assays To examine the properties of the tumors grown by AGE, G361 cells were added to plastic dishes (Nunc, Naperville, IL) coated with purified collagen I. After 18 h, cells were photographed under phase contrast microscopy. The spreading cells were counted as spindle cells if they had a length/width ratio greater than 3. In a transmigration assay, the upper side of a modified Boyden chamber polycarbonate membrane (Transwell 24, 8-μm pore, Costar, Cambridge, MA) (Albini *et al*, 1987) either was left uncoated (transmigration) or was coated (invasion) with Matrigel (1 mg/mL) (Matrigel-GFR, Falcon-Becton Dickinson, Bedford, MA) for 2 h at room temperature (Kleinman *et al*, 1986). Cells were then seeded in the upper chambers in their respective culture medium without fetal bovine serum but containing AGE, and incubated for either 16 h (transmigration) or 48 h (invasion) at 37°C. The chambers were fixed and stained with crystal violet. The cells on the lower surface of the filter were counted (two fields/well) using a microscope with a × 10 objective. Each condition was assayed in triplicate, and each experiment was repeated at least three times.

Tumor growth *in vivo* Experiments to determine the effect of anti-RAGE antibodies on G361 tumor growth were performed in Balb/c-nu/nu mice. Cultured G361 cells were washed and resuspended in PBS; subsequently 5×10^6 cells (suspended in 0.1 mL of PBS) were injected subcutaneously into the upper flank of 6-wk-old female athymic nude mice (n = 5/group). Mice received intraperitoneal injections of 0.3 mL of control IgG (0.5 mg) or anti-RAGE antibodies (0.5 mg) 10 d later and from then on once every 5 days. Tumor size was estimated on day 30 using orthogonal linear measurements made with Vernier calipers according to the formula volume (mm^3) = [(width, mm)^2 × (length, mm)]/2. This experiment was repeated twice with similar results. Blood vessels in the tumor were visualized by CD34 staining, which was performed on cryosections using the fluorescein isothiocyanate-conjugated rat anti-mouse CD34 (PharMingen, San Diego, CA). Nuclei were stained with propidium iodide.

Survival and in vivo metastasis assays A single-cell suspension of 1×10^6 G361 cells was injected into the peritoneal cavity of 6-wk-old female athymic nude mice (n = 5/group). Mice received intraperitoneal injections of 0.3 mL of control IgG (0.5 mg) or anti-RAGE antibodies (0.5 mg) 10 d later and from then every 5 d. Mice were then observed for survival, which was recorded as the percentage of surviving animals over time (in days) after tumor injection. To measure the spontaneous metastasis, 1×10^6 cells were injected into the upper flank of 6-wk-old athymic nude mice (n = 5/group). When the mean tumor volume reached 500 mm^3, primary tumors were removed. Mice were then maintained for an additional 3 wk to allow further growth and development of lung metastases. Mice received intraperitoneal injections of 0.3 mL of control IgG (0.5 mg) or anti-RAGE antibodies (0.5 mg) once every 3 d after tumors were removed. The mice were necropsied, and the lungs were removed. Visible lung metastases were counted with the aid of a dissecting microscope.

Immunohistochemical staining Serial paraffin sections were immunostained according to the standard streptavidin-biotin peroxidase technique using a Vectastain ABC elite kit (Vector Laboratories). After incubation with 10% goat serum to eliminate nonspecific binding, these sections were followed by incubation overnight at 4°C with the primary antibodies diluted 1:500 to 1:1000 in PBS. The sections were then sequentially incubated with the biotinylated secondary antibody. Then the sections were counterstained with hematoxylin.

Statistical analysis The data were statistically analyzed for significance by Student's t test, except for the *in vivo* survival assays, which were analyzed using Wilcoxon analysis.

We thank Ms Ayumi Honda for excellent technical assistance and Dr James R. McMillan for his manuscript proofreading.

DOI: 10.1046/j.0022-202X.2004.22218.x

Manuscript received April 10, 2003; revised August 29, 2003; accepted for publication September 9, 2003

Address correspondence to: Riichiro Abe, MD, PhD, Department of Dermatology, Hokkaido University Graduate School of Medicine, N 15 W 7, Kita-ku, Sapporo 060-8638, Japan. Email: aberi@med.hokudai.ac.jp

References

Albini A, Iwamoto Y, Kleinman HK, Martin GR, Aaronson SA, Kozlowski JM, McEwan RN: A rapid *in vitro* assay for quantitating the invasive potential of tumor cells. Cancer Res 47:3239–3245, 1987

Ikeda K, Higashi T, Sano H, *et al*: N (epsilon)-(carboxymethyl) lysine protein adduct is a major immunological epitope in proteins modified with advanced glycation end products of the Maillard reaction. Biochemistry 35:8075–8083, 1996

Kislinger T, Fu C, Huber B, *et al*: (epsilon)-(carboxymethyl) lysine adducts of proteins are ligands for receptor for advanced glycation end products that activate cell signaling pathways and modulate gene expression. J *Biol Chem* 274:31740–31749, 1999

Kleinman HK, McGarvey ML, Hassell JR, Star VL, Cannon FB, Laurie GW, Martin GR: Basement membrane complexes with biological activity. Biochemistry 25:312–318, 1986

Ling X, Sakashita N, Takeya M, Nagai R, Horiuchi S, Takahashi K: Immunohistochemical distribution and subcellular localization of three distinct specific molecular structures of advanced glycation end products in human tissues. Lab Invest 78:1591–1606, 1998

Masaki H, Okano Y, Sakurai H: Generation of active oxygen species from advanced glycation end-products (AGE) under ultraviolet light A (UVA) irradiation. *Biochem Biophys Res Commun* 235:306–310, 1997

McKie RM: Incidence, risk factors and prevention of melanoma. Eur J Cancer 34:S3–S6, 1998

Mizutari K, Ono T, Ikeda K, Kayashima K, Horiuchi S: Photo-enhanced modification of human skin elastin in actinic elastosis by N (epsilon)-(carboxymethyl) lysine, one of the glycoxidation products of the Maillard reaction. J Invest Dermatol 108:797–802, 1997

Morton DL, Wong JH, Kikwood JM, Parker RG: Cancer medicine. In: Holland JF, Frei E, Bast RC (eds). Malignant Melanoma, 3rd ed. Philadelphia: Lea & Febiger, 1993; p 1793–1824

Mullarkey CJ, Edelstein D, Brownlee M: Free radical generation by early glycation products: A mechanism for accelerated atherogenesis in diabetes. Biochem Biophys Res Commun 173:932–939, 1990

Noonan FP: Neonatal sunburn and melanoma in mice. Nature 413:271–272, 2001

Sasaki N, Fukatsu R, Tsuzuki K, *et al*: Advanced glycation end products in Alzheimer's disease and other neurodegenerative diseases. *Am J Pathol* 153:1149–1155, 1998

Sasaki N, Toki S, Chowei H, *et al*: Immunohistochemical distribution of the receptor for advanced glycation end products in neurons and astrocytes in Alzheimer's disease. Brain Res 888:256–262, 2001

Schmidt AM, Yan SD, Yan SF, Stern DM: The multiligand receptor RAGE as a progression factor amplifying immune and inflammatory responses. J Clin Invest 108:949–955, 2001

Setlow R, Grist E, Thompson K, Woodhead AD: Wavelengths effective in induction of malignant melanoma. Proc Natl Acad Sci USA 90:6666–6670, 1993

Shimizu T, Abe R, Nakamura H, Ohkawara A, Suzuki M, Nishihira J: High expression of macrophage migration inhibitory factor in human melanoma cells and its role in tumor cell growth and angiogenesis. Biochem Biophys Res Commun 264:751–758, 1999

Stitt AW, Li YM, Gardiner TA, Bucala R, Archer DB, Vlassara H: Advanced glycation end products (AGE) co-localize with AGE receptors in the retinal vasculature of diabetic and of AGE-infused rats. Am J Pathol 150:523–531, 1997

Taguchi A, Blood DC, del Toro G, *et al*: Blockade of RAGE-amphoterin signaling suppresses tumour growth and metastases. Nature 405:354–360, 2000

Takeuchi M, Bucala R, Suzuki T, *et al*: Neurotoxicity of advanced glycation end-products for cultured cortical neurons. J Neuropathol Exp Neurol 59:1094–1105, 2000a

Takeuchi M, Makita Z, Bucala R, Suzuki T, Koike T, Kameda Y: Immunological evidence that non-carboxymethyllysine advanced glycation end-products are produced from short chain sugars and dicarbonyl compounds *in vivo*. Mol Med 6:114–125, 2000b

Takeuchi M, Makita Z, Yanagisawa K, Kameda Y, Koike T: Detection of noncarboxymethyllysine and carboxymethyllysine advanced glycation end products (AGE) in serum of diabetic patients. Mol Med 5:393–405, 1999

Tanaka N, Yonekura H, Yamagishi S, Fujimori H, Yamamoto Y, Yamamoto H: The receptor for advanced glycation end products is induced by the glycation products themselves and tumor necrosis factor-alpha through nuclear factor-kappa B, and by 17beta-estradiol through Sp-1 in human vascular endothelial cells. J Biol Chem 275:25781–25790, 2000

Tanji N, Markowitz GS, Fu C, *et al*: Expression of advanced glycation end products and their cellular receptor RAGE in diabetic nephropathy and nondiabetic renal disease. J Am Soc Nephrol 11:1656–1666, 2000

Yamagishi S, Yonekura H, Yamamoto Y, *et al*: Advanced glycation end products-driven angiogenesis *in vitro*: Induction of the growth and tube formation of human microvascular endothelial cells through autocrine vascular endothelial growth factor. J Biol Chem 272:8723–8730, 1997

Yamamoto Y, Yamagishi S, Hsu CC, Yamamoto H: Advanced glycation endproducts–receptor interactions stimulate the growth of human pancreatic cancer cells through the induction of platelet-derived growth factor-B. Biochem Biophys Res Commun 213:681–687, 1995

Yang CW, Vlassara H, Peten EP, He CJ, Striker GE, Striker LJ: Advanced glycation end products up-regulate gene expression found in diabetic glomerular disease. Proc Natl Acad Sci USA 91:9436–9440, 1994

Yonekura H, Yamamoto Y, Sakurai S, *et al*: RAGE engagement and vascular cell derangement by short chain-derived advanced glycation endproducts. In: Horiuchi S (ed). International Congress Series 1245. Amsterdam: Elsevier Science, 2002; p 129–135

American Journal of Pathology, Vol. 164, No. 4, April 2004

Overexpression of Pigment Epithelium-Derived Factor Decreases Angiogenesis and Inhibits the Growth of Human Malignant Melanoma Cells *in Vivo*

Riichiro Abe,* Tadamichi Shimizu,* Sho-ichi Yamagishi,† Akihiko Shibaki,* Shinjiro Amano,† Yosuke Inagaki,† Hirokazu Watanabe,* Hiroshi Sugawara,* Hideki Nakamura,* Masayoshi Takeuchi,‡ Tsutomu Imaizumi,† and Hiroshi Shimizu*

From the Department of Dermatology, Hokkaido University Graduate School of Medicine, Sapporo; the Department of Medicine,† Kurume University School of Medicine, Kurume; and the Department of Biochemistry,‡ Faculty of Pharmaceutical Science, Hokuriku University, Kanazawa, Japan*

Pigment epithelium-derived factor (PEDF) has recently been shown to be the most potent inhibitor of angiogenesis in the mammalian eye, and is involved in the pathogenesis of angiogenic eye disease such as proliferative diabetic retinopathy. However, a functional role for PEDF in tumor growth and angiogenesis remains to be determined. In this study, we have investigated both the *in vitro* and *in vivo* growth characteristics of human malignant melanoma G361 cell lines, stably transfected to overexpress human PEDF. Expression levels of PEDF proteins in melanoma cell lines G361 and A375 were comparable with that of human cultured melanocytes, whereas vascular endothelial growth factor levels in two tumor cell lines were much stronger than that in normal melanocytes. Overexpression of PEDF was found to significantly inhibit tumor growth and vessel formation in G361 nude mice xenografts. Furthermore, *in vitro* proliferation rates of G361 cells were decreased in PEDF-transfected cells. PEDF proteins showed dose-dependent induced growth retardation and apoptotic cell death in nontransfected G361 cells, which were completely prevented by treatment with antibodies against the Fas ligand. Our present study highlights two beneficial effects of PEDF treatment on melanoma growth and expansion; one is the suppression of tumor angiogenesis, and the other is induction of Fas ligand-dependent apoptosis in tumor cells. PEDF therefore might be a promising novel therapeutic agent for treatment of patients with melanoma. *(Am J Pathol 2004, 164:1225–1232)*

Angiogenesis, a process by which new vascular networks are formed from pre-existing capillaries, is required for tumors to grow, invade, and metastasize.[1,2] Tumors are unable to grow beyond a volume of 1 to 2 mm^3 without establishing a vascular supply because cells must be within 100 to 200 μm of a blood vessel to survive.[1,2] Tumor vessels are genetically stable, and less likely to accumulate mutations that allow them to develop drug resistance in a rapid manner.[3] Therefore, targeting vasculatures that support tumor growth, rather than cancer cells, is considered the most promising approach to cancer therapy.

Pigment epithelium-derived factor (PEDF), a glycoprotein that belongs to the superfamily of serine protease inhibitors, was first purified from human retinal pigment epithelial cell-conditioned media as a factor with potent human retinoblastoma cell neuronal differentiating activity.[4] Recently, PEDF has been shown to be a potent inhibitor of angiogenesis in both cell culture and animal models. Indeed, PEDF is reported to inhibit retinal endothelial cell growth and migration and suppress ischemia-induced retinal neovascularization.[5,6] Furthermore, loss of PEDF was associated with angiogenic activity in proliferative diabetic retinopathy.[7] However, a functional role for PEDF in tumor growth and angiogenesis remains to be elucidated.

In this study, we investigated both *in vitro* and *in vivo* growth characteristics of the human malignant melanoma cell line G361, stably transfected to overexpress human PEDF.

Materials and Methods

Cells and Mice

Two human malignant melanoma cell lines G361 and A375 (American Type Culture Collection, Manassas, VA) were maintained in RPMI 1640 supplemented with 10% fetal calf serum, 100 U/ml penicillin/streptomycin. Normal

Supported in part by the Japan Society for the Promotion of Science (grants-in-aid for scientific research to H.S. and R.A.); and the Ministry of Education, Culture, Sports, Science, and Technology, Japan (grants of Venture Research and Development Centers to S.Y.).

Accepted for publication December 10, 2003.

Address reprint requests to Riichiro Abe, M.D., Ph.D., Department of Dermatology, Hokkaido University Graduate School of Medicine, N 15 W 7, Kita-ku, Sapporo 060-8638, Japan. E-mail: aberi@med.hokudai.ac.jp.

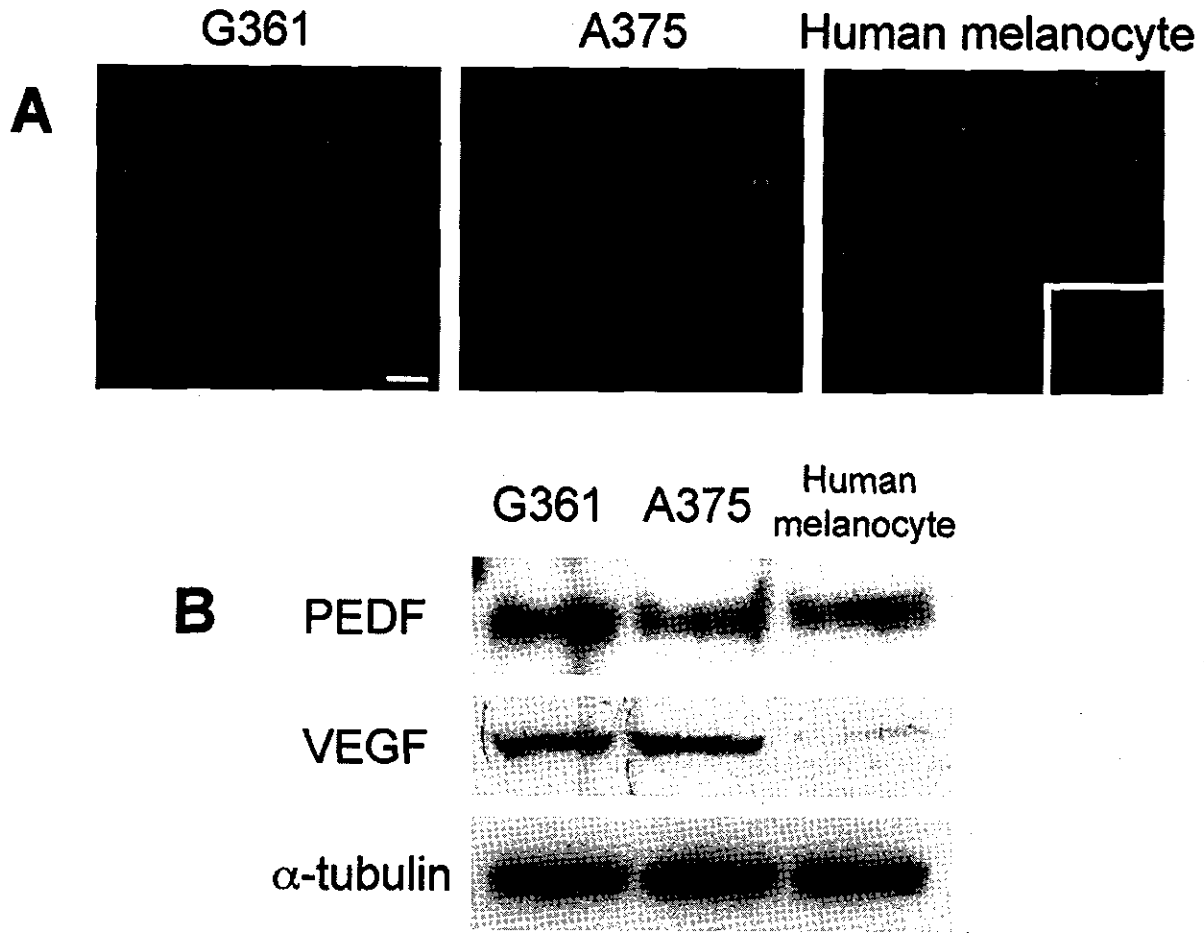

Figure 1. Immunofluorescence staining (**A**) and Western blot analysis (**B**) of G361, A375, and normal melanocytes. **A:** Immunofluorescence staining for PEDF was performed as described in Materials and Methods. The **inset** indicates negative staining without primary antibody. **B:** Expression levels of PEDF, VEGF, and α-tubulin in cell lysates were analyzed as described in Materials and Methods. Scale bar, 10 μm.

human neonatal melanocytes were purchased from Kurabo (Osaka, Japan) and maintained according to the manufacturer's instructions.

BALB/c-nu/nu mice were purchased from Japan Clea (Tokyo, Japan) and maintained under specific pathogen-free conditions. All animal procedures were conducted according to guidelines provided by the Hokkaido University Institutional Animal Care and Use Committee under an approved protocol.

Preparation of Polyclonal Antibodies against Human PEDF

Polyclonal antibody against 44-mer PEDF peptides (VLLSPLSVATALSALSLGAEQRTESIIHRALYYDLISSFDIHGT) was prepared as previously described.[8] We confirmed that the polyclonal antibody actually bound to purified PEDF protein (data not shown).

Immunofluorescence Microscopy

Immunofluorescence staining was performed on G361, A375, or normal melanocytes cultured on glass coverslips. Each cell type was incubated with an anti-PEDF antibody at 4°C overnight, and then these primary antibodies were detected with fluorescein isothiocyanate-labeled goat anti-rabbit IgG (Vector Laboratories, Burlingame, CA). Fluorescence staining was detected using a confocal laser-scanning fluorescence microscope (Laser Scanning Confocal Imaging System MRC 1024; Bio-Rad, Richmond, CA).

Construction of PEDF Expression Vector

PEDF cDNA was originally cloned from a human placenta cDNA library (Clontech, Palo Alto, CA), and inserted into the mammalian expression vector pBK-CMV (Stratagene, La Jolla, CA) as described previously.[8]

Purification of PEDF Proteins

293T cells (American Type Culture Collection, Rockville, MD) were transfected with a PEDF expression vector using the FuGENE 6 transfection reagent (Roche Diagnostics, Mannheim, Germany) according to the manufacturer's instructions. Then PEDF proteins were purified

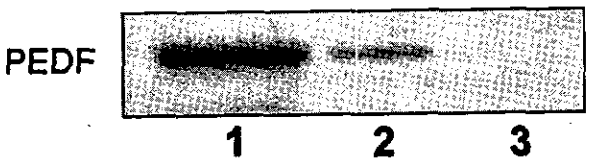

Figure 2. Western blot analysis of conditioned medium from G361 cells, stably transfected with the human PEDF expression vector (**lane 2**) or with the expression vector alone (**lane 3**). Purified PEDF proteins (0.2 μg) were used as a positive control (**lane 1**).

from conditioned media by a Ni-NTA spin kit (Qiagen GmbH, Hilden, Germany) according to the manufacture's instructions. Sodium dodecyl sulfate-polyacrylamide gel electrophoresis analysis of purified PEDF proteins revealed a single band with a molecular weight of ~50 kd, which showed reactivity with the previously described antibody against human PEDF.[8]

Selection of Stable Transfectants Overexpressing PEDF

Subconfluent G361 or A375 cultures were stably transfected either with a PEDF expression vector or with an expression vector alone using the FuGENE 6 transfection reagent. Twenty-four hours after transfection, cells were split 1:3 into their full growth medium containing 400 μg/ml of Zeocin (Invitrogen, Carlsbad, CA) to select transfectants. Stably transfected clones were expanded, and the clones were characterized for PEDF production.

Western Blot Analysis

G361, A375, and normal melanocytes were grown to confluence in 100-mm dishes, washed with phosphate-buffered saline (PBS), and lysed as previously described.[9] Conditioned medium was obtained from stably transfected G361 cells grown for 48 hours in serum-free culture medium, and then concentrated 20-fold using Microcon 10 MWCO filters (Amicon, Beverly, MA). Proteins were electrophoresed on polyacrylamide gels under reducing conditions, and then blotted onto nitrocellulose filters. Filters were blocked with nonfat dried milk and followed by incubation with a primary antibody against human PEDF, human vascular endothelial growth factor (VEGF) (Santa Cruz Biotechnology, Santa Cruz, CA), or α-tubulin (Santa Cruz Biotechnology). After incubation, the filters were treated with horseradish peroxidase-conjugated anti-rabbit IgG (Amersham Pharmacia Biotech, Piscataway, NJ), and the resultant immune complexes were visualized using an enhanced chemiluminescence detection system (ECL) (Amersham) as previously described.[8]

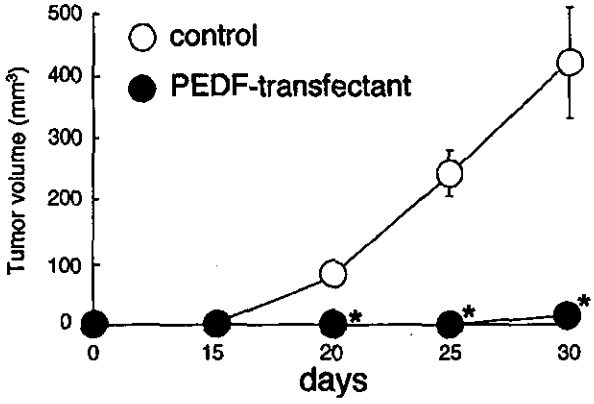

Figure 3. Growth of G361 xenografts in nude mice. G361 cells, stably transfected with the human PEDF expression vector or with the expression vector alone, were injected intradermally into the flanks of five 6-week-old female athymic nude mice. The tumor volumes were calculated as described in Materials and Methods. *, $P < 0.0001$ compared with control cells.

Growth of G361 Xenografts in Nude Mice

Confluent G361 cells, stably transfected with the human PEDF expression vector or with the expression vector alone, were trypsinized and resuspended in PBS at a density of 1×10^7 cells/ml. One million tumor cells were injected intradermally into the flanks of each 6-week-old female athymic nude mouse ($n = 5$). The smallest and largest diameters of the tumors were measured after a 5-day interval using a pair of digital calipers, and the tumor volumes were calculated using the following formula: volume (mm^3) = [(smallest diameter)^2 × (largest diameter)]/2.[10]

Immunofluorescence Staining of Tumor Vessels

To determine the degree of tumor-induced angiogenesis, cryostat sections were prepared from tumor xenografts 30 days after implantation. Five cryostat sections of each tumor xenograft were stained with fluorescein isothiocyanate-conjugated rat anti-mouse CD31 (PharMingen, San Diego, CA). Nuclei were stained with propidium iodide. Three different fields at ×60 magnification were examined on each section using a confocal laser-scanning fluorescence microscopy. The percentage of fluorescent-positive areas in three different fields from each section was measured.

Cell Growth and Apoptosis Assays

G361 cells, stably transfected with the human PEDF expression vector or with the expression vector alone, were serum-starved for 24 hours, and cell numbers were counted at days 2, 4, and 6 using a dye exclusion method. To investigate effects of PEDF proteins on the growth and apoptosis of nontransfected G361 cells, the cells were incubated with or without various concentrations of PEDF proteins in the presence or absence of 10 μg/ml of monoclonal antibody against Fas ligand (PharMingen). After 6 days of incubation, viable cell numbers were determined. Apoptosis was measured with an enzyme-linked immunosorbent assay for DNA fragments after a 16-hour incubation according to the manufactur-

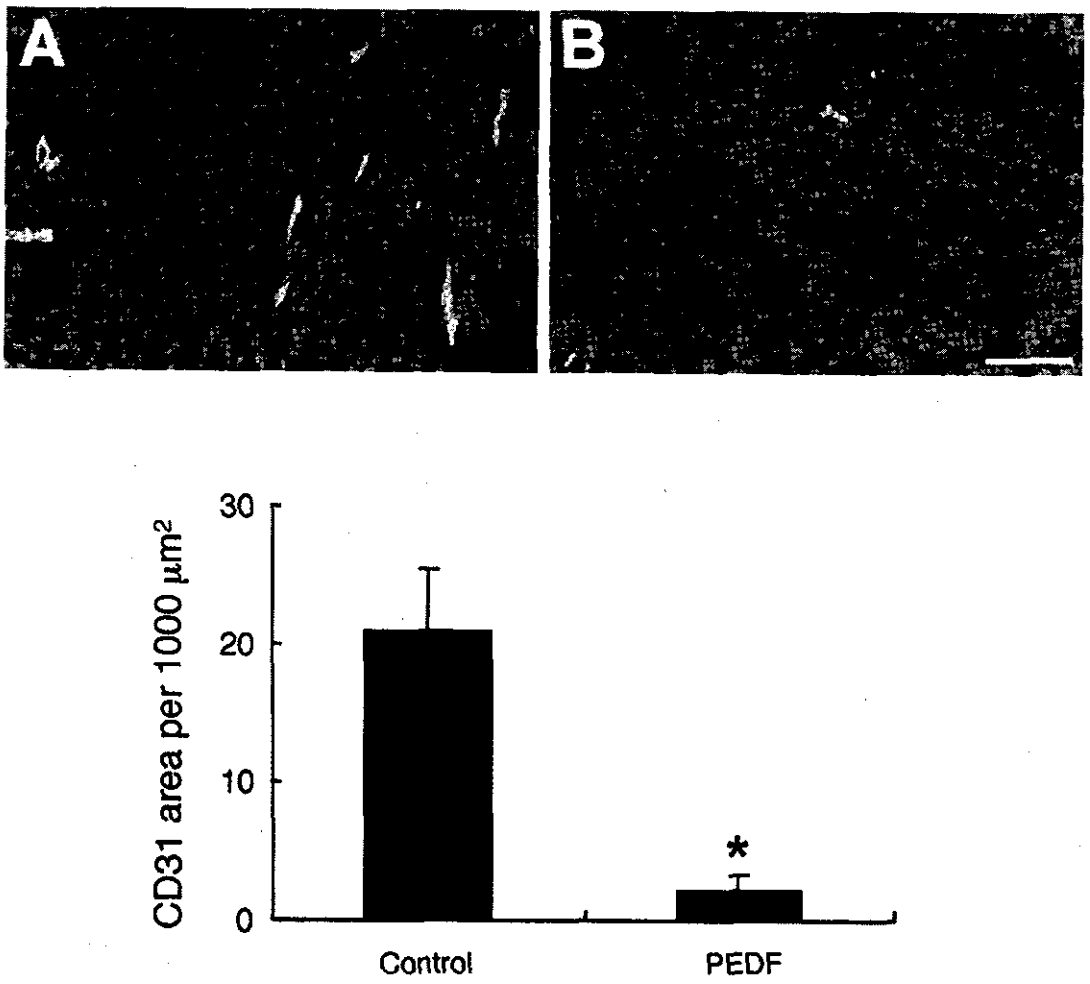

Figure 4. Tumor vessels in G361 xenografts. Typical photomicrographs of immunofluorescent staining for CD31 (green) in G361 xenografts. Nuclei were stained with propidium iodide (red). G361 cells, stably transfected with the human PEDF expression vector (**A**) or with the expression vector alone (**B**). **Bottom**: The quantitative analysis of the fluorescent-positive area (per 1000 μm^2) in tumors. *, $P < 0.0001$ compared to control cells. Scale bar, 50 μm.

er's instructions (Cell Death Detection ELISA; Roche Molecular Biochemicals, Mannheim, Germany).

Assay for in Situ *Apoptosis*

To determine the degree of apoptosis, cryostat sections were prepared from tumor xenografts 30 days after implantation. Terminal dUTP nick-end labeling (TUNEL) assay was performed using *in situ* apoptosis detection kit (Boehringer Mannheim, Mannheim, Germany). The number of apoptotic cells was counted in 10 randomly selected fields at ×200 magnification using an immunofluorescence microscope.

Statistical Analysis

All values were presented as means ± SEM (standard error of the mean). Statistical significance was evaluated using the Student's *t*-test for paired comparison; $P < 0.05$ was considered significant.

Results

PEDF and VEGF Expression by Melanoma Cells and Normal Melanocytes

The human malignant melanoma cell lines G361 and A375 were chosen for their endogenous expression of PEDF and VEGF. As shown in Figure 1, A and B, G361 and A375 cells were found to express substantial amounts of PEDF, and the expression levels of PEDF in these tumor cells were comparable with that of normal human cultured melanocytes. In contrast, expression levels of VEGF among these cells were quite different; G361 and A375 cells were characterized by a strong expression of VEGF, whereas little VEGF protein was detected in cell lysates from normal melanocytes (Figure 1B).

Next, we investigated the expression levels of PEDF proteins in the G361 cell-conditioned medium that were stably transfected with the human PEDF expression vector. As shown in Figure 2, PEDF-transfected G361 cells

secreted increased amounts of PEDF, whereas control vector-transfected cells expressed little or no supernatant PEDF proteins. PEDF-transfected A375 cells showed similar results (data not shown).

Growth of PEDF-Overexpressing G361 Cells in Vivo

Next, we examined whether PEDF overexpression influences the tumor growth of G361 cells *in vivo*. As shown in Figure 3, control vector-transfected cells formed rapidly growing tumors, reaching 300 to 400 mm^3 after 30 days. In contrast, PEDF overexpression almost completely inhibited *in vivo* tumor growth of G361 cells throughout this observation period of up to 30 days (Figure 3).

Tumor Vessels in PEDF-Overexpressing G361 Xenografts

To determine the tumor-induced angiogenesis within PEDF-transfected and control vector-transfected tumors, five different frozen sections from each tumor were stained with an antibody against mouse CD31. As shown in Figure 4, morphometric analysis revealed decreased tumor vessels in 30-day-old tumors derived from the PEDF-overexpressing G361 cells, compared with control vector-transfected tumor cells.

Growth and Apoptosis of G361 Cells in Vitro

To determine whether PEDF overexpression influences tumor cell proliferation *in vitro*, we measured growth rates of cultured G361 cells, stably transfected with a human PEDF expression vector or with the expression vector alone. As shown in Figure 5A, growth rates of PEDF transfectants were significantly lower than that of control vector-transfected cells. Furthermore, PEDF proteins dose dependently retarded growth and induced apoptotic cell death in cultured nontransfected G361 cells, which was completely blocked by treatments with a neutralizing antibody against Fas ligand (Figure 5, B and C). These results suggest that PEDF elicits apoptosis in G361 cells indirectly, in a Fas ligand-dependent manner.

Apoptosis in PEDF-Overexpressing G361 Xenografts

Finally, we examined apoptosis in the PEDF-transfected and control vector-transfected tumors, frozen sections from each tumor were analyzed using TUNEL assay. As shown in Figure 6, apoptotic cells were significantly increased in the tumors derived from the PEDF-overexpressing G361 cells, compared with control vector-transfected tumor cells.

Discussion

A major event in tumor growth and expansion is the angiogenic switch, an alteration in the balance of proangiogenic and anti-angiogenic molecules that leads to tumor neovascularization.[1] Indeed, many tumors, including malignant melanoma not only overexpress multiple angiogenic factors such as VEGF, basic fibroblast growth factor, and interleukin-8, but also underexpress angiogenic inhibitors such as thrombospondin-1, thus favoring

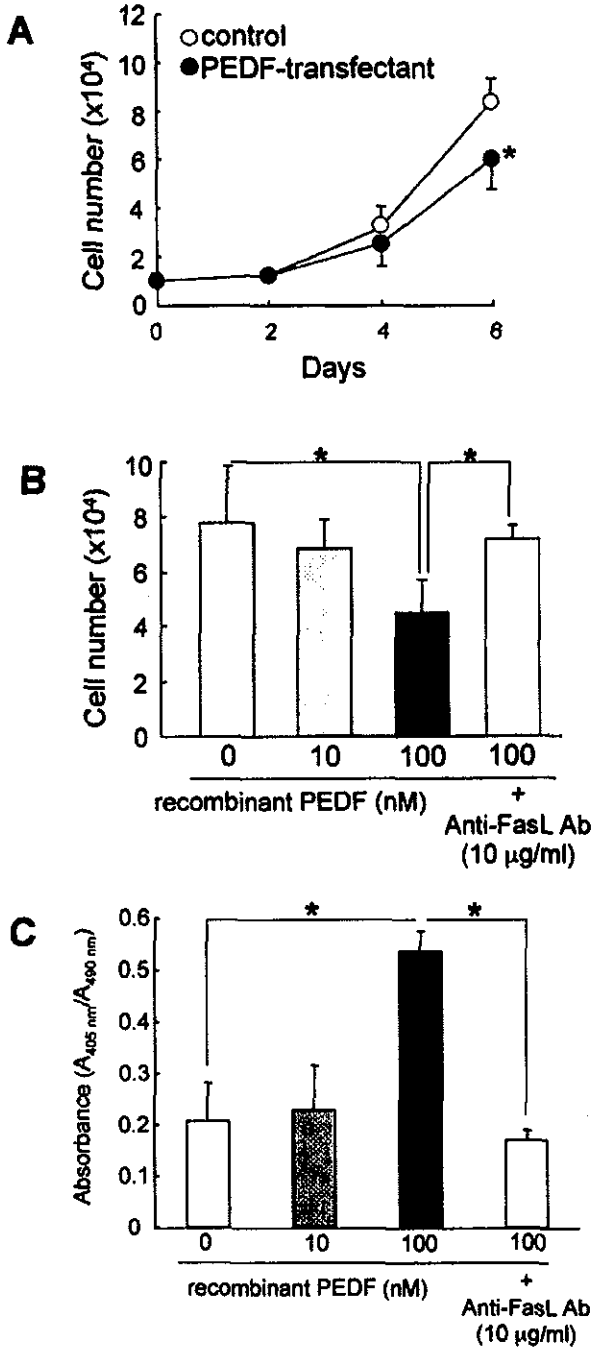

Figure 5. Growth and apoptosis of G361 cells *in vitro*. **A:** Growth rates of G361 cells, stably transfected with the human PEDF expression vector or with the expression vector alone *in vitro*. Growth (**B**) and apoptosis (**C**) of nontransfected G361 cells. Cells were incubated with or without the indicated concentrations of PEDF proteins in the presence or absence of 10 μg/ml of monoclonal antibody against Fas ligand. *, $P < 0.005$ compared to the value without treatments.

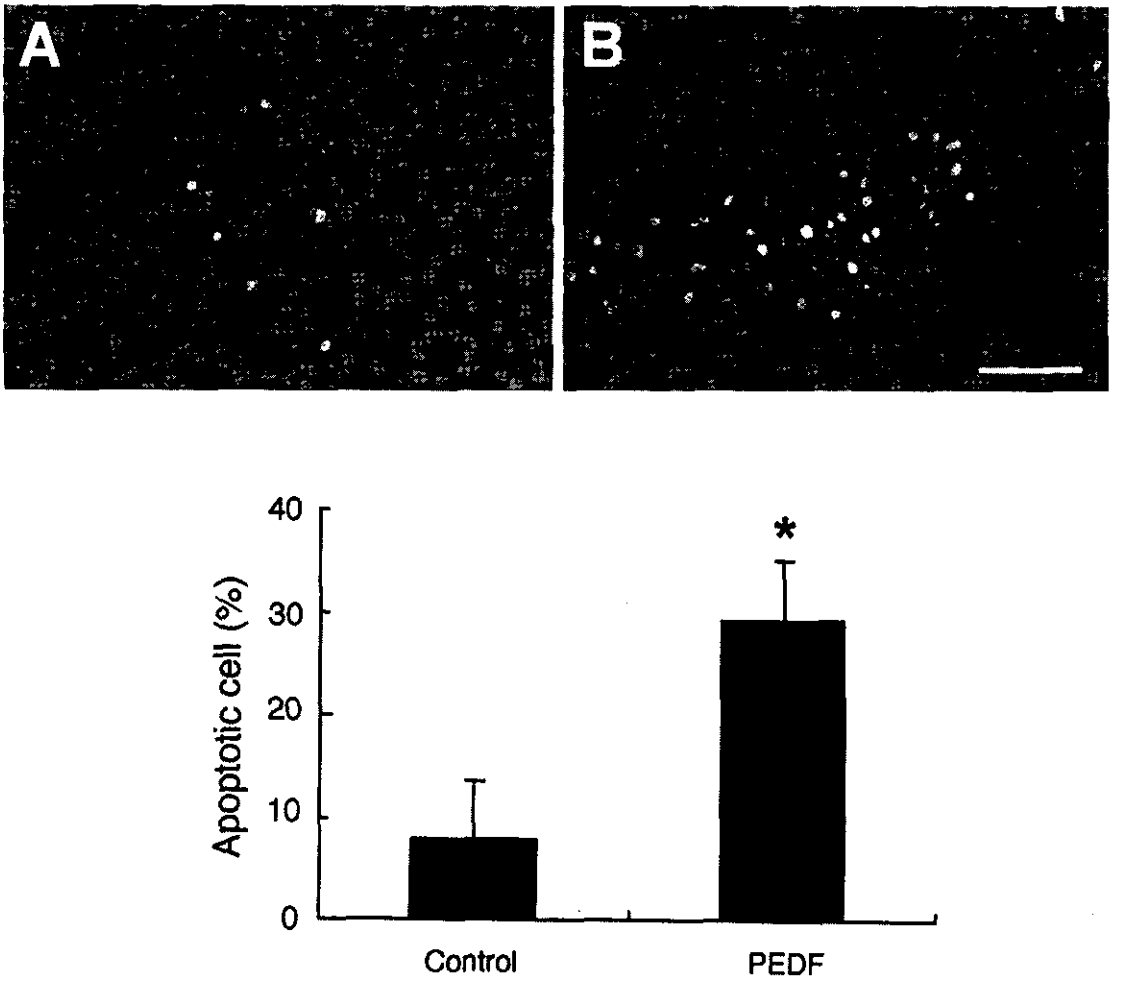

Figure 6. Apoptotic cells in G361 xenografts. Typical photomicrographs of apoptotic cells using TUNEL assay (green) in G361 xenografts. Nuclei were stained with propidium iodide (red). G361 cells, stably transfected with the human PEDF expression vector (**A**) or with the expression vector alone (**B**). **Bottom:** The quantitative analysis of the apoptotic cell percentage in tumors. *, $P < 0.005$ compared to control cells. Scale bar, 50 μm.

angiogenesis.[11,12] In this study, we demonstrated for the first time that two human malignant melanoma cell lines, G361 and A375, expressed substantial amounts of PEDF protein and that the expression levels of PEDF in cell lysates were comparable with that of normal (nonmalignant) human melanocytes. The present observations suggest that a decrease or loss in PEDF production alone might not contribute to malignant melanoma development. To elucidate the physiological roles of PEDF derived from normal melanocytes in skin would be beyond the original scope of this study. However, recently, others and we have shown that PEDF protected retinal vascular and neuronal cells from oxidative stress-induced injury.[8,13] Because H_2O_2 is formed as a byproduct of melanin synthesis, after ultraviolet irradiation in mammalian skin, PEDF secreted by melanocytes might be involved in the maintenance of normal skin homeostasis through its anti-oxidative properties.[14] In this study we found that two melanoma cell lines express high levels of VEGF proteins, whereas normal melanocytes produced a minimal amount of VEGF. Melanocytes are transformed to malignant melanoma cells by constitutive signal activation via a mitogen-activated protein kinase, a process that is associated with an increase in production of VEGF, supporting the hypothesis for a functional role of VEGF in melanoma transformation.[15]

In this present study, we found for the first time that overexpression of PEDF decreases tumor angiogenesis and almost completely inhibits the growth of G361 melanoma xenografts in nude mice. PEDF is also known to effectively suppress retinal and choroidal neovascularization caused by ischemia and age-related macular degeneration, respectively.[6,16] Very recently, Doll and colleagues[17] reported that PEDF inhibits stromal vasculature and epithelial tissue growth, mediating an anticancer effect for pancreas cancer. Blocking tumor vascularization using PEDF may also be a promising approach for melanoma treatment. Previous studies have shown that malignant melanoma responds well to antiangiogenic therapy using other endogenous angiogenic inhibitors such as angiostatin (plasminogen kringles 1 to 4) and endostatin.[18,19] Because plasminogen kringle 5 was recently reported to inhibit ischemia-induced retinal neovascularization in a rat model by down-regulating

VEGF and up-regulating PEDF,[20] the anti-angiogenic and growth inhibitory effects of angiostatin on melanoma cells could be ascribed, at least in part, to this PEDF activity.

It is possible that the concentrations used in these present studies (up to 100 nmol/L) were beyond the normal physiological concentrations, and the inhibitory effect was nonspecific toxicity. However previous studies have shown, for example, complete inhibition of vessel formation that was obtained at a concentration of ~50 nmol/L.[21] In addition, the estimated human blood concentration of PEDF is 100 nmol/L, which is a functionally significant concentration of PEDF in our studies, indicating that the blood circulation itself holds the capacity to inhibit angiogenesis in tissues throughout the entire body.[22] Therefore the PEDF concentrations in our experiments may not be too high and remain within the parameters found under normal physiological conditions. Furthermore, we experimented the assay for *in situ apoptosis* to determine whether exogenous PEDF within tumor induces apoptosis. We could show that apoptotic cells were significantly increased in the tumors derived from the PEDF-overexpressing G361 cells, compared with control vector-transfected tumor cells (Figure 6). This result suggested that the endogenous PEDF in our animal model was not physiologically at too high a level to induce nonspecific toxicity, because nonspecific toxicity resulted in necrosis.

Here, we have been the first to identify a PEDF-induced growth retardation and induction of apoptotic cell death in melanoma cells that is dependent on the Fas ligand. PEDF up-regulates Fas ligand in endothelial cells, thereby specifically sensitizing tumor vessels to apoptosis.[23] PEDF could directly elicit apoptosis in G361 cells by inducing Fas ligand on these tumor cells. Recently, granulocytes have been shown to inhibit melanoma lung metastasis by inducing Fas ligand-associated apoptosis, further supporting this speculation.[24]

Our present study has highlighted two beneficial aspects of the effects of PEDF on melanoma growth and expansion; one is the suppression of tumor angiogenesis, and the other is induction of Fas ligand-dependent apoptosis in tumor cells. PEDF is therefore a promising novel therapeutic agent for treatment of patients with certain types of cancer including melanoma.

Acknowledgments

We thank Ms. Ayumi Honda and Ms. Maki Goto for their excellent technical assistance and Dr. James R. McMillan for his manuscript proofreading.

References

1. Holmgren L, O'Reilly MS, Folkman J: Dormancy of micrometastases: balanced proliferation and apoptosis in the presence of angiogenesis suppression. Nat Med 1995, 1:149–153
2. Carmeliet P, Jain RK: Angiogenesis in cancer and other diseases. Nature 2000, 407:249–257
3. Scappaticci FA: Mechanisms and future directions for angiogenesis-based cancer therapies. J Clin Oncol 2002, 20:3906–3927
4. Tombran-Tink J, Chader CG, Johnson LV: PEDF: a pigment epithelium-derived factor with potent neuronal differentiative activity. Exp Eye Res 1991, 53:411–414
5. Dawson DW, Volpert OV, Gillis P, Crawford SE, Xu HJ, Benedict W, Bouck NP: Pigment epithelium-derived factor: a potent inhibitor of angiogenesis. Science 1999, 285:245–248
6. Duh EJ, Yang HS, Suzuma I, Miyagi M, Youngman E, Mori K, Katai M, Yan L, Suzuma K, West K, Davarya S, Tong P, Gehlbach P, Pearlman J, Crabb JW, Aiello LP, Campochiaro PA, Zack DJ: Pigment epithelium-derived factor suppresses ischemia-induced retinal neovascularization and VEGF-induced migration and growth. Invest Ophthalmol Vis Sci 2002, 43:821–829
7. Spranger J, Osterhoff M, Reimann M, Mohlig M, Ristow M, Francis MK, Cristofalo V, Hammes HP, Smith G, Boulton M, Pfeiffer AF: Loss of the antiangiogenic pigment epithelium-derived factor in patients with angiogenic eye disease. Diabetes 2001, 50:2641–2645
8. Yamagishi S, Inagaki Y, Amano S, Okamoto T, Takeuchi M, Makita Z: Pigment epithelium-derived factor protects cultured retinal pericytes from advanced glycation end product-induced injury through its antioxidative properties. Biochem Biophys Res Commun 2002, 296: 877–882
9. Shimizu T, Abe R, Nakamura H, Ohkawara A, Suzuki M, Nishihira J: High expression of macrophage migration inhibitory factor in human melanoma cells and its role in tumor cell growth and angiogenesis. Biochem Biophys Res Commun 1999, 264:751–758
10. Taetle RF, Rosen I, Abramson J, Venditti S, Howell S: Use of nude mouse xenografts as preclinical drug screens: in vivo activity of established chemotherapeutic agents against melanoma and ovarian carcinoma xenografts. Cancer Treat Rep 1987, 71:297–304
11. Rofstad EK, Halsør EF: Vascular endothelial growth factor, interleukin 8, platelet-derived endothelial cell growth factor, and basic fibroblast growth factor promote angiogenesis and metastasis in human melanoma xenografts. Cancer Res 2000, 60:4932–4938
12. Reiher FK, Volpert OV, Jimenez B, Crawford SE, Dinney CP, Henkin J, Haviv F, Bouck NP, Campbell SC: Inhibition of tumor growth by systemic treatment with thrombospondin-1 peptide mimetics. Int J Cancer 2002, 98:682–689
13. Cao W, Tombran-Tink J, Chen W, Mrazek D, Elias R, McGinnis JF: Pigment epithelium-derived factor protects cultured retinal neurons against hydrogen peroxide-induced cell death. J Neurosci Res 1999, 57:789–800
14. Jimenez-Cervantes C, Martinez-Esparza M, Perez C, Daum N, Solano F, Garcia-Borron JC: Inhibition of melanogenesis in response to oxidative stress: transient downregulation of melanocyte differentiation markers and possible involvement of microphthalmia transcription factor. J Cell Sci 2001, 114:2335–2344
15. Govindarajan B, Bai X, Cohen C, Zhong H, Kilroy S, Louis G, Moses M, Arbiser JL: Malignant transformation of melanocytes to melanoma by constitutive activation of mitogen-activated protein kinase kinase (MAPKK) signaling. J Biol Chem 2003, 278:9790–9795
16. Holekamp NM, Bouck N, Volpert O: Pigment epithelium-derived factor is deficient in the vitreous of patients with choroidal neovascularization due to age-related macular degeneration. Am J Ophthalmol 2002, 134:220–227
17. Doll JA, Stellmach VM, Bouck NP, Bergh AR, Lee C, Abramson LP, Cornwell ML, Pins MR, Borensztajn J, Crawford SE: Pigment epithelium-derived factor regulates the vasculature and mass of the prostate and pancreas. Nat Med 2003, 9:774–780
18. Rodolfo M, Cato EM, Soldati S, Ceruti R, Asioli M, Scanziani E, Vezzoni P, Parmiani G, Sacco MG: Growth of human melanoma xenografts is suppressed by systemic anglostatin gene therapy. Cancer Gene Ther 2001, 8:491–496
19. Scappaticci FA, Contreras A, Smith R, Bonhoure L, Lum B, Cao Y, Engleman EG, Nolan GP: Statin-AE: a novel angiostatin-endostatin fusion protein with enhanced antiangiogenic and antitumor activity. Angiogenesis 2001, 4:263–268
20. Gao G, Li Y, Gee S, Dudley A, Fant J, Crosson C, Ma JX: Down-regulation of vascular endothelial growth factor and up-regulation of pigment epithelium-derived factor: a possible mechanism for the anti-angiogenic activity of plasminogen kringle 5. J Biol Chem 2002, 277:9492–9497
21. Stellmach V, Crawford SE, Zhou W, Bouck N: Prevention of ischemia-

induced retinopathy by the natural ocular antiangiogenic agent pigment epithelium-derived factor. Proc Natl Acad Sci USA 2001, 98: 2593–2597
22. Petersen SV, Valnickova Z, Enghild JJ: Pigment-epithelium-derived factor (PEDF) occurs at a physiologically relevant concentration in human blood: purification and characterization. Biochem J 2003, 374:199–206
23. Volpert OV, Zaichuk T, Zhou W, Reiher F, Ferguson TA, Stuart PM, Amin M, Bouck NP: Inducer-stimulated Fas targets activated endothelium for destruction by anti-angiogenic thrombospondin-1 and pigment epithelium-derived factor. Nat Med 2002, 8:349–357
24. Chen YL, Wang JY, Chen SH, Yang BC: Granulocytes mediates the Fas-L-associated apoptosis during lung metastasis of melanoma that determines the metastatic behaviour. Br J Cancer 2002, 87:359–365

Journal of Dermatological Science (2004) 35, 154–157

ELSEVIER

Journal of Dermatological SCIENCE

www.intl.elsevierhealth.com/journals/jods

LETTER TO THE EDITOR

Remodeling of desmosomal and hemidesmosomal adhesion systems during human hair follicle development

Complex cell–cell and cell–extracellular matrix interactions are implied in the induction and promotion of hair follicle morphogenesis. Desmosomes (DS) and hemidesmosomes (HD) are thought to play important roles in the signal transduction during the regulation of cell growth and differentiation. Recently, remodeling of these two cell adhesion systems was suggested to underlie hair follicle morphogenesis in mouse pelage hair follicles [1]. Mindful of this hypothesis, we speculated that remodeling of DS and HD are involved in the regulation of cell growth and differentiation during human hair follicle morphogenesis. In the present study, we investigated the expression of major DS and HD components and the ultrastructural formation of DS and HD in the developing human hair follicles of skin samples from human fetuses from a series of estimated gestational ages (EGA) (49–163 days EGA).

Human embryonic and fetal skin specimens were obtained through the Central Laboratory of Human Embryology at the University of Washington, Seattle, USA with the approval of the Human Subjects Review Board and in accordance with the United States DHEW policies. The ages, the autopsy sites, and the numbers of embryos or fetuses were as follows: 49–64 days EGA, scalp ($n = 2$), trunk ($n = 2$); 65–84 days EGA, scalp ($n = 3$), trunk ($n = 2$); 85–104 days EGA, scalp ($n = 2$), trunk ($n = 2$); 105–135 days EGA, scalp ($n = 2$), trunk ($n = 2$); >135 days EGA, scalp ($n = 2$), trunk ($n = 2$). EGA was determined from maternal histories, fetal measurements (crown rump and foot length) and comparative histological appearance of epidermis.

Immunofluorescent studies to detect the expression of DS and HD components were performed as described previously [2], using primary antibodies as follows; mouse monoclonal anti-desmogleins 1 and 2 antibody (DG3.10) (Progen Biotechnik GmbH, Heidelberg, Germany), mouse monoclonal anti-desmoglein 3 antibody (5H10) [3], mouse monoclonal anti-plakoglobin antibody (4F11) (produced by Prof. Margaret J. Wheelock), mouse monoclonal anti-desmoplakins 1 and 2 antibody (2.15) (Progen Biotechnik GmbH), mouse monoclonal anti-β4 integrin antibody (1A3) [4], mouse monoclonal anti-BPAG2 antibody (D20) [5], rabbit polyclonal anti-BPAG1 antibody (S1193) [6], mouse monoclonal anti-plectin (HD1) antibody (HD-121) [7].

In the hair germ (65–84 days EGA), the inner cells showed strong membranous immunoreactivity for all the three DS components, desmoglein 3, plakoglobin and desmoplakins 1 and 2, as shown in the intermediate cells in the interfollicular epidermis. The expression of all three DS components was weaker in the outer layer basal cells in contact with the basement membrane (BM) than that in the inner cells. In the hair peg (85–104 days EGA), the membrane associated pattern of staining was seen for all the DS components, although again the staining was weak in the outermost layer cells in contact with BM (Fig. 1a). In the bulbous hair peg (105–135 days EGA) and the differentiated lanugo hair follicle (>135 days EGA), the DS components were expressed throughout the entire hair follicle, although the outermost layer of the outer root sheath, the bulge cells and the matrix cells showed only weak expression of the DS components (Fig. 1b and c). Ultrastructurally, the outermost layer of the developing hair follicle in contact with BM exhibited only a small number of DS in any stage of development. The number of DS seen in the inner cells having no contact with BM was similar to that of the intermediate cell layers in the interfollicular epidermis, except that the bulge cells and the matrix cells showed only a smaller number of DS.

Basically, a similar DS component expression patterns to that of in the interfollicular epidermis was seen in the developing hair follicle throughout hair follicle morphogenesis, i.e., the expression was stronger in the cells that had no contact with the BM compared to the cells in contact with the BM (Fig. 2a–c). However, the bulge cells and matrix cells were the exception as they only weakly expressed DS components even though they failed to have any contact with the BM. Considering the fact that the bulge is thought to be an enriched source of hair follicle stem cells [8], the fact that most cells in the fetal bulge including the inner cells showed only weak DS components staining

0923-1811/$30.00
doi:10.1016/j.jdermsci.2004.03.006

demonstrates the immature nature of bulge cells and suggests similarity with a stem cell phenotype.

As for HD components, positive staining for β4 integrin, BPAG1, BPAG2 and plectin (HD1), were continuously observed along the BM of the hair germ. HD components were present in BM continuously from the interfollicular epidermis to the mid-portion of the hair peg (Fig. 1d). At the tip of the distal end of the hair peg, the HD staining was weak or negative. In the bulbous hair peg (105–135 days EGA) and the differentiated lanugo hair follicle (>135 days EGA), HD components were continuously expressed along the BM from the interfollicular epidermis to mid-portion between the bulge and the bulb (Fig. 1e and f). HD components were absent from the BM of the bulb region, although the expression of HD components were seen in the area between the matrix cells and the dermal papilla cells. Morphological HD formation was confirmed in the BM of the hair germ, the upper part of the hair peg, the bulge region and the upper part of the bulbous hair peg and the late hair follicle. Morphological HD formation in the bulge of the developing human hair follicle has been previously reported [9].

In the present study, a reduction in the formation of HDs was shown at the tip (lower portion) of the hair peg. In fact, it was suggested that digestion of type VII collagen, a major component of anchoring fibril, by matrilysin (MMP-7) and gelatinase A (MMP-2) produced by the mesenchymal-like cells in the developing dermis plays a significant role during the

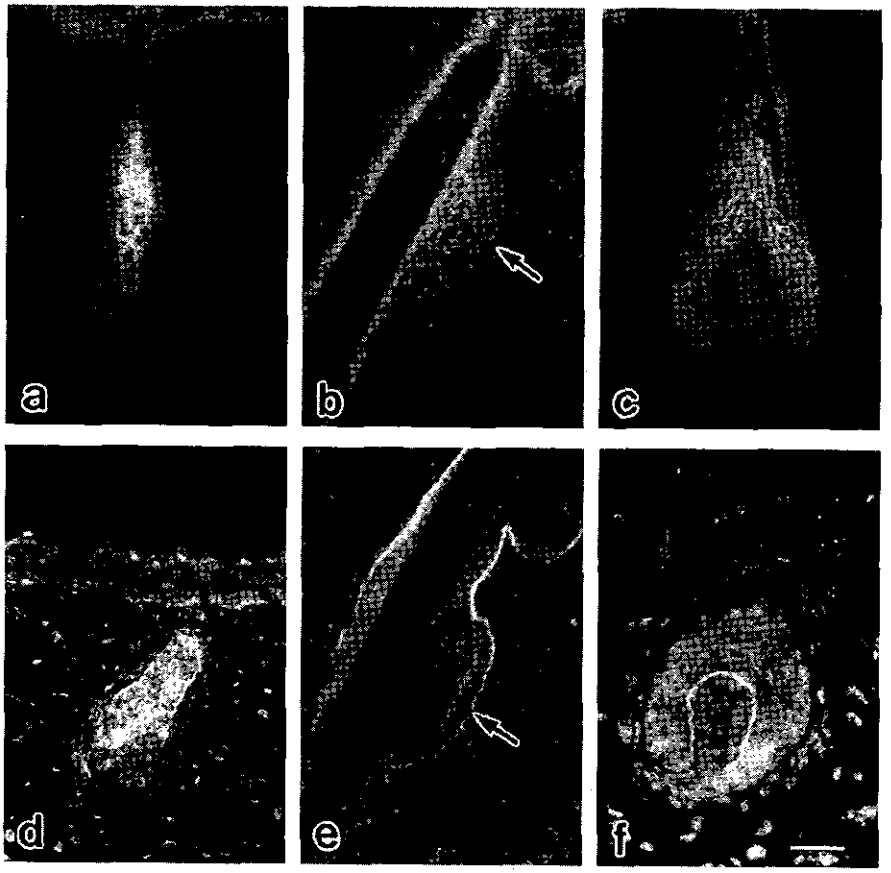

Fig. 1 Desmosome (DS) components were strongly expressed in the inner portion, and hemidesmosome (HD) components were expressed in the upper portion including the bulge region of the developing hair follicles. Strong immunoreactivity for DS components was seen in the inner cells of the hair peg (a, desmogleins 1 and 2), although the staining was weak in most of bulge cells (arrow) (b, desmoplakins 1 and 2) and matrix cells (c, plakoglobin). Staining for HD components was lost at the tip of the hair peg (d, BPAG2), but remerged in the bulge region (arrow) (e, BPAG2) and between the matrix cells and the dermal papilla (f, β4 integrin). Immunostaining was demonstrated with fluorescein isothiocyanate (FITC, green) and the nuclear stain was done with propidium iodide (red). Yellowish color was the result of an overlap of FITC fluorescence and propidium iodide fluorescence and partly by nonspecific detection of FITC fluorescence by the filter for propidium iodide. (a, d) hair peg, (b, c, e, f) differentiated lanugo hair follicle. Bar, 50 μm.

invasion of developing hair follicles into the dermis [10]. Our present findings further support the notion that a reduction in HD adhesion may be a part of the follicle elongation process in the developing hair peg.

Putative stem cells were thought to be sequentially localized to the entire hair germ, to the outermost cells of hair peg, and finally settled in the bulge and the outermost layer of the outer root sheath in the bulbous hair peg and in the differentiated lanugo hair follicle [2]. From our present results, HD components would appear to always be expressed at the sites of putative stem cells including the bulge during human hair follicle morphogenesis (Fig. 2).

Based on plural lines of evidence, the hair follicle bulge is thought to be an indispensable pool of stem cells [8]. Concerning to this bulge, type IV and type VII collagen have been reported to be persistently expressed in the BM of the bulge region throughout human hair follicle morphogenesis [9]. These BM observations including our present results imply that the HD mediated cell–extracellular matrix adhesion may be involved in maintaining and stabilizing the stem cell pool within the bulge area.

HD and BM components were also strongly expressed between the matrix cells and the dermal papilla in the bulb region of the differentiated hair follicle. This finding suggests that the HD and BM components may be important for the cell growth of the transient amplifying cells in the matrix region during human hair follicle morphogenesis.

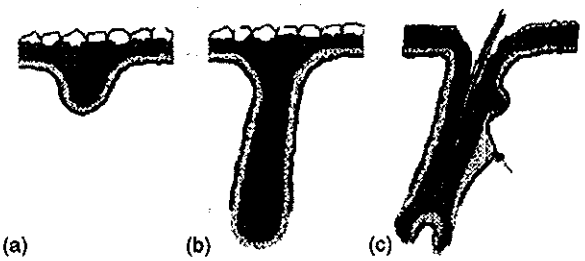

Fig. 2 Schematic illustration of the sequential expression of desmosome (DS) and hemidesmosome (HD) molecules during human fetal hair follicle development. Different expression levels for the two categories of molecules are represented by different levels of dot density (for DS components) or continuous or dotted lines (for HD components). (a) hair germ (65–84 days EGA), (b) hair peg (85–104 days EGA), (c) bulbous hair peg (105–135 days EGA) and differentiated lanugo hair follicle (>135 days EGA). *Arrows*, bulge.

Acknowledgements

We thank Prof. John Stanley for providing us the antibody S1193; Prof. Margaret J. Wheelock for providing us the antibodies, 5H10 and 4F11; Prof. Katsushi Owaribe for a kind gift of the antibodies, D20 and 1A3; Prof. John E. Olerud, Ms. Marcia L. Usui and Mr. Robert A. Underwood for providing us with the human fetal skin specimens; Ms. Keiko Hatanaka, Ms. Yuriko Okuno and Ms. Megumi Sato for their fine technical assistance on this project.

References

[1] Nanba D, Hieda Y, Nakanishi Y. Remodeling of desmosomal and hemidesmosomal adhesion systems during early morphogenesis of mouse pelage hair follicles. J Invest Dermatol 2000;114:171–7.
[2] Akiyama M, Smith LT, Shimizu H. Changing patterns of localization of putative stem cells in developing human hair follicles. J Invest Dermatol 2000;114:321–7.
[3] Proby CM, Ota T, Suzuki H, Koyasu S, Gamou S, Shimizu N, et al. Development of chimeric molecules for recognition and targeting of antigen-specific B cells in pemphigus vulgaris. *Br J Dermatol* 2000;142:321–30.
[4] Hirako Y, Usukura J, Uematsu J, Hashimoto T, Kitajima Y, Owaribe K. Cleavage of BP180, a 180-kDa bullous pemphigoid antigen, yields a 120-kDa collagenous extracellular polypeptide. J Biol Chem 1998;273:9711–7.
[5] Nishizawa Y, Uematsu J, Owaribe K. HD4, a 180 kDa bullous pemphigoid antigen, is a major transmembrane glycoprotein of the hemidesmosome. J Biochem (Tokyo) 1993;113: 493–501.
[6] Tanaka T, Korman NJ, Shimizu H, Eady RA, Klaus-Kovtun V, Cehrs K, et al. Production of rabbit antibodies against carboxy-terminal epitopes encoded by bullous pemphigoid cDNA. J Invest Dermatol 1990;94:617–23.
[7] Hieda Y, Nishizawa Y, Uematsu J, Owaribe K. Identification of a new hemidesmosomal protein, HD1: a major, high molecular mass component of isolated hemidesmosomes. J Cell Biol 1992;116:1497–506.
[8] Lavker RM, Sun TT, Oshima H, Barrandon Y, Akiyama M, Ferraris C, et al. Hair follicle stem cells. J Invest Dermatol Symp Proc 2003;8:28–38.
[9] Akiyama M, Dale BA, Sun T-T, Holbrook KA. Characterization of hair follicle bulge in human fetal skin; the human fetal bulge is a pool of undifferentiated keratinocytes. J Invest Dermatol 1995;105:844–50.
[10] Karelina TV, Bannikov GA, Eisen AZ. Basement membrane zone remodeling during appendageal development in human fetal skin. The absence of type VII collagen is associated with gelatinase-A (MMP2) activity. J Invest Dermatol 2000;114:371–5.

Masashi Akiyama*
Daisuke Sawamura
Hiroshi Shimizu
Department of Dermatology, Hokkaido University Graduate School of Medicine, North 15 West 7

Kita-ku, Sapporo 060-8638
Japan

Itsuro Matsuo
Department of Dermatology
Teikyo University School of Medicine
Ichihara Hospital, Ichihara 299-0111
Japan

*Corresponding author
Tel.: +81-11-716-1161x5962
fax: +81-11-706-7820
E-mail address: akiyama@med.hokudai.ac.jp
(M. Akiyama)

26 February 2004